Resistive switching characteristic and uniformity of low-power HfO_x-based resistive random access memory with the BN insertion layer*

Shuai Su(苏帅), Xiao-Chuan Jian(鉴肖川), Fang Wang(王芳)†, Ye-Mei Han(韩叶梅), Yu-Xian Tian(田雨仙), Xiao-Yang Wang(王晓旸), Hong-Zhi Zhang(张宏智), and Kai-Liang Zhang(张楷亮)‡

School of Electronics Information Engineering, Tianjin Key Laboratory of Film Electronic & Communication Devices, Tianjin University of Technology, Tianjin 300384, *China*

(Received 6 May 2016; revised manuscript received 22 June 2016; published online 25 August 2016)

In this letter, the Ta/HfO_x/BN/TiN resistive switching devices are fabricated and they exhibit low power consumption and high uniformity each. The reset current is reduced for the HfO_x/BN bilayer device compared with that for the Ta/HfO_x/TiN structure. Furthermore, the reset current decreases with increasing BN thickness. The HfO_x layer is a dominating switching layer, while the low-permittivity and high-resistivity BN layer acts as a barrier of electrons injection into TiN electrode. The current conduction mechanism of low resistance state in the HfO_x/BN bilayer device is space-charge-limited current (SCLC), while it is Ohmic conduction in the HfO_x device.

Keywords: resistive random access memory (RRAM), low-power consumption, uniformity, HfO_x

PACS: 73.40.Rw, 85.30.–z, 85.35.–p **DOI:** 10.1088/1674-1056/25/10/107302

1. Introduction

Metal-oxide-based resistive random access memory (RRAM) is one of the most promising candidates for next-generation non-volatile memory applications due to its simple metal–insulator–metal (MIM) sandwich structure, great scalability potential, fast switching speed, Complementary Metal Oxide Semiconductor (CMOS) compatibility, etc.[1–5] Because of these superior characteristics, a number of metal oxides, such as HfO_x, WO_x, TiO_x, VO_x have been reported for RRAM applications.[6–11] Among these metal oxides, the HfO_x-based RRAMs are especially attractive for their excellent switching properties. However, there are several problems that need to be solved from the angle of practical application, such as the high operational current and large resistive switching fluctuation, which have been the major barriers for mass storage applications.

To reduce power consumption, several methods have been proposed, such as using device area scaling and bilayer structure.[12,13] In order to improve the resistive switching memory uniformity, some efforts have been made, such as doping and employing bilayer structure[14–16] in the memory devices and so on. BN film is a wide bandgap semiconductor material and it has high resistivity, low dielectric constant and low dielectric loss, which can be a candidate as insert layer for resistive memory devices.

In this paper, an effective method is proposed to reduce the reset current and improve the distribution of the resistive switching parameters by using HfO_x/BN bilayer structure, which is made by using the insertion of the low permittivity and high resistivity BN layer between the HfO_x layer and TiN bottom electrode.

2. Experiment

Ta/HfO_x/BN/TiN and Ta/HfO_x/TiN devices were fabricated. 100-nm TiN bottom electrode (BE) was deposited on SiO_2/Si substrates by using directive current (DC) reactive magnetron sputtering. The embedded layer, 2-, 4-, 6-, 8-nm BN thin films were deposited on TiN/SiO_2/Si substrates by radio frequency (RF) magnetron sputtering with BN ceramic target separately. The sputtering was carried out in $Ar + N_2$ mixed gas ambient (Ar/N_2 = 30 sccm/2 sccm) with a working pressure of 0.8 Pa at room temperature. The HfO_x (200 nm) resistive switching layer was deposited on the BN thin film at room temperature by using RF magnetron sputtering. Then the Ta top electrode with 300 μm in diameter was deposited with the aid of a shadow mask and the Ta/HfO_x/BN/TiN devices were obtained. For comparison, the Ta/HfO_x/TiN devices were fabricated under the same deposition condition.

Electrical characterizations were performed by using Agilent B1500A semiconductor device analyzer at room temperature. A positive bias was applied to the Ta top electrode, while the TiN bottom electrode was grounded for all mea-

*Project supported by the National Natural Science Foundation of China (Grant Nos. 61274113, 11204212, 61404091, 51502203, and 51502204), the Tianjin Natural Science Foundation, China (Grant Nos. 14JCZDJC31500 and 14JCQNJC00800), and the Tianjin Science and Technology Developmental Funds of Universities and Colleges, China (Grant No. 20130701).

†Corresponding author. E-mail: fwang75@163.com

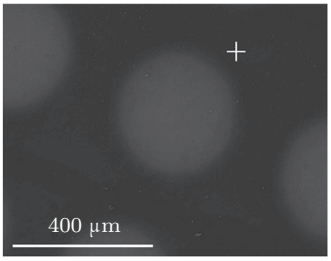
‡Corresponding author. E-mail: kailiang_zhang@163.com

© 2016 Chinese Physical Society and IOP Publishing Ltd

surements in this paper. An energy dispersive x-ray detector (EDX) was employed to detect the element composition and relative atomic percent within the HfO_x/BN/TiN thin film.

3. Results and discussion

The element composition and relative atomic percentage of HfO_x/BN/TiN thin film is observed by using an energy dispersive x-ray detector (EDX). As shown in Fig. 1, atomic percentage of O, Hf, Ti, N, B, C, and Si is 13.11:0.58:8.15:10.05:5.43:6:56.68, and the presence of these elements corresponds to the TiN, HfO, BN in the prepared device. As figure 2 shows, the FTIR spectrum of the BN exhibits a spectral band centred at 1360 cm^{-1}, which is attributed to adsorption band of h-BN. The FTIR characteristic peak of h-BN combined with the EDX results confirms the existence of BN thin film. Figure 3 gives the AFM image (1 μm×1 μm) of BN, the surface is smooth and particles are uniform.



Element	Weight percent	Atom percent
B K	2.29	5.43
C K	2.81	6.00
N K	5.48	10.05
O K	8.17	13.11
Si K	62.02	56.68
Ti K	15.21	8.15
Hf M	4.03	0.58

Fig. 1. EDX spectrum within HfO_x/BN/TiN thin film.

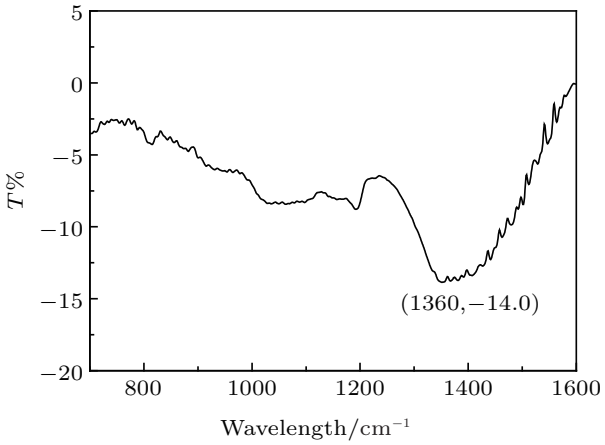


Fig. 2. FT–IR spectra of the BN film.

Figure 4(a) shows the resistive switching characteristics in the Ta/HfO_x/TiN structure with 100-μA compliance current. There is no resistive switching phenomenon after ten continuous cycles.

Figure 4(b) shows the typical bipolar resistive switching characteristics of the Ta/HfO_x/TiN structure with 1mA compliance current. When the positive electric field is applied to the Ta electrode, the electrons from TiN electrode are injected into HfO_x layer, which leads to the formation of oxygen vacancy filament. The device is transformed into LRS from

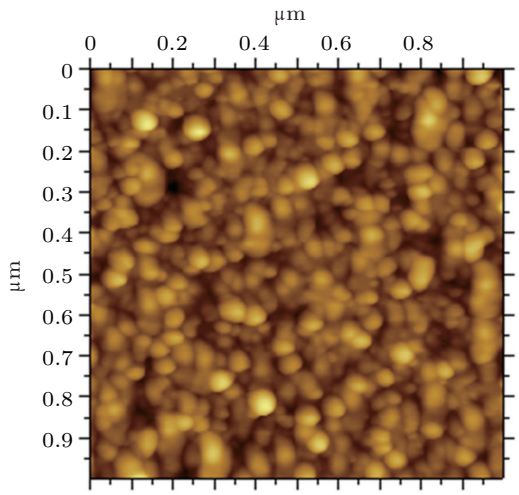


Fig. 3. (color online) AFM images (1 μm×1 μm) of BN.

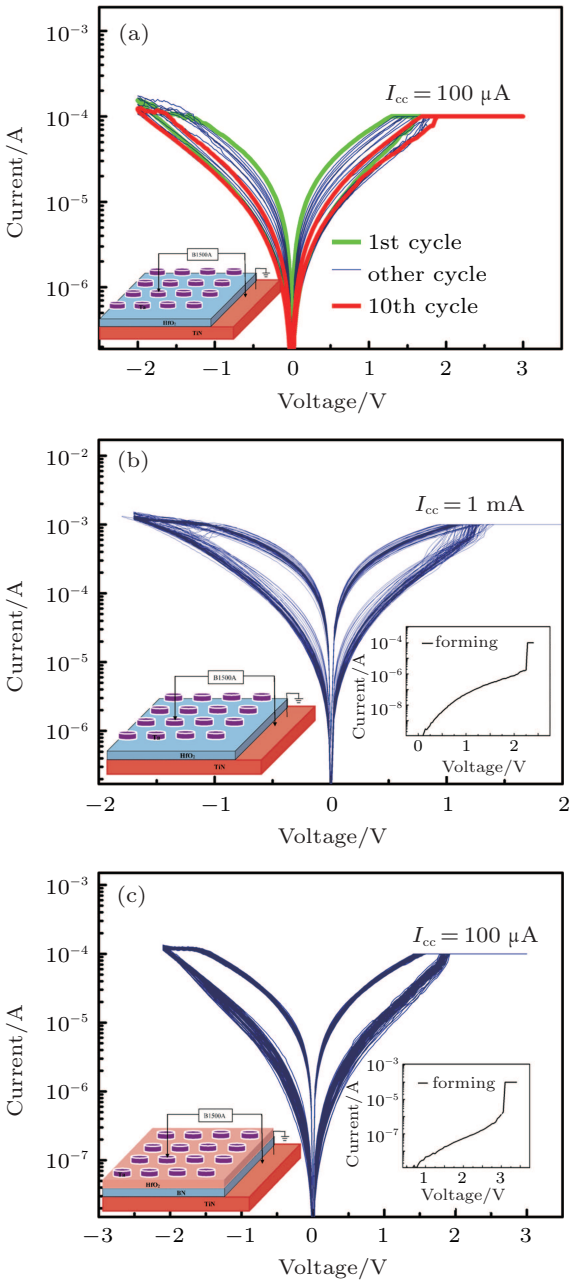


Fig. 4. (color online) Typical bipolar DC *I–V* characteristics in Ta/HfO_x/TiN device [(a) and (b)] and Ta/HfO_x/BN/TiN device (c).

HRS, and the set process occurs. When the negative electric field is applied to the Ta electrode, the electrons from HfO_x layer are injected into TiN electrode, and the oxygen vacancy filaments are broken. The device is transformed into HRS from LRS, and the reset process occurs. Thus, we believe that the resistive switching process of the device is controlled by the electric field applied to the Ta electrode. Note that, the forming process (as shown in the inset) is required to activate the following resistive switching cycles. Wide distributions from 0.96 V to 1.62 V are found for set voltages (V_{set}) during the DC sweeping operations. The maximum reset current is shown to be more than 1 mA.

Figure 4(c) exhibits the continuous I–V curves of set and reset processes in Ta/HfO_x/BN/TiN structure. In the set process, the electrons pass through BN barrier layer from TiN electrode and are injected into HfO_x layer. In the reset process, the electrons pass through BN barrier layer from HfO_x layer and are injected into TiN electrode. It can be clearly noticed that the distribution of the switching cycles is greatly minimized and the maximum reset current is pronouncedly reduced by more than one order.

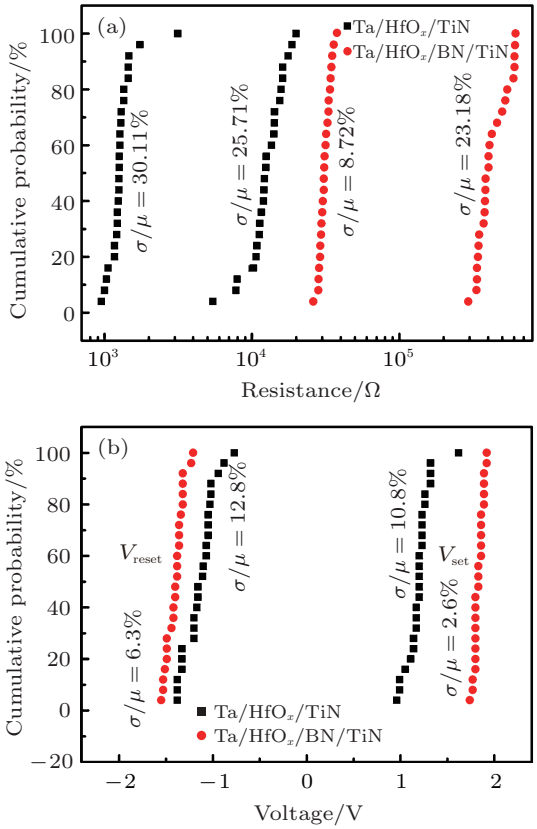


Fig. 5. (color online) Statistical distributions of (a) HRS and LRS (b) V_{set} and V_{reset} in the 100 continuous switching cycles for Ta/HfO_x/TiN device and Ta/HfO_x/BN/TiN device.

Figure 5 indicates the distributions of HRS, LRS, and set voltage (V_{set}), reset voltage (V_{reset}) during continuous 100 DC sweeping cycles for the Ta/HfO_x/TiN and Ta/HfO_x/BN/TiN samples. μ is the mean value and σ is the standard deviation, while σ/μ refers to the relative fluctuation (defined by the standard deviation divided by the mean value). The relative fluctuations of HRS and LRS in the Ta/HfO_x/TiN devices are 25.71% and 30.11%, while relative fluctuations of HRS and LRS for Ta/HfO_x/BN/TiN devices are 23.18% and 8.72%, respectively as shown in Fig. 5(a). The relative fluctuations of V_{set} and V_{reset} for the Ta/HfO_x/TiN devices are 10.8% and 12.8%. However, after inserting a thin BN layer, the relative fluctuations for V_{set} and V_{reset} can be reduced to 2.6% and 6.3%, respectively as shown in Fig. 5(b). It is suggested that the inclusion of a thin BN layer can also improve the uniformity of the device. As reported previously, the low permittivity BN layer with very smooth surface is likely to act as a concentrated electric field, which restricts the conduction path[17] and improves resistive switching uniformity.

In addition, the Ta/HfO_x/BN/TiN device could retain better reliability. Figure 6 exhibits the variations of the HRS and LRS with time for the Ta/HfO_x/BN/TiN device at 85 °C. After 10^4 s, there is no degradation observed in HRS ($\sim 3.16 \times 10^5$ Ω) nor LRS ($\sim 2.35 \times 10^4$ Ω). Furthermore, the reset current decreases with BN thickness increasing from 0 nm to 8 nm as shown in Fig. 7, the BN film between the TiN bottom electrode and HfO_2 resistive layer is likely to act as a barrier layer which hinders the electron injection, as a result, oxygen vacancies are reduced and the resistance of LRS is increased, and thus the reset current is reduced.

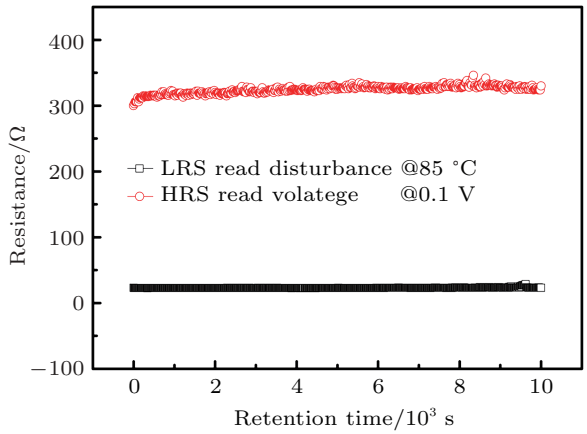


Fig. 6. (color online) Retention test under 0.1 V read bias for 10^4 s at 85 °C for the Ta/HfO_x/BN/TiN device.

In order to investigate the resistive switching phenomena in the Ta/HfO_x/TiN and Ta/HfO_x/BN/TiN devices, the measured curves of ln(I) versus ln(V) are plotted. As shown in Figs. 8(a) and 8(b), the I–V curve fitting shows that the current conductions in the LRS of the single HfO_x and bilayer HfO_x/BN devices are dominated by Ohmic conduction and space-charge-limited current (SCLC),[18] respectively, which might be attributed to the insertion of low-permittivity and

high-resistivity BN layer between the HfO_x layer and TiN bottom electrode.

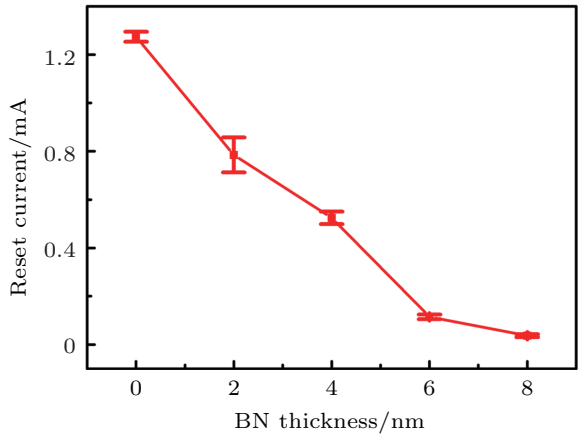


Fig. 7. (color online) Reset current versus BN thickness.

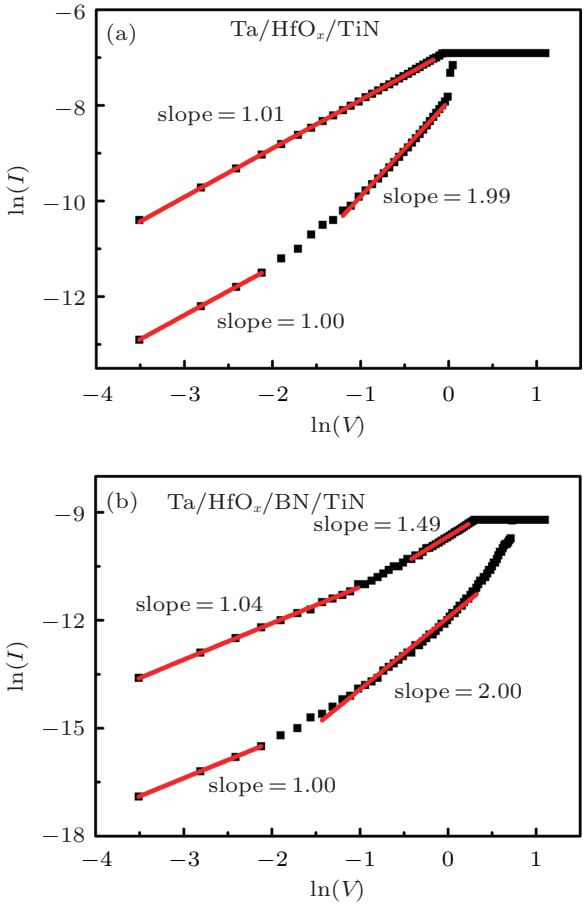


Fig. 8. (color online) (a) Plots of ln(I) versus ln(V) in LRS and HRS of the HfO_x device; (b) a plot of ln(I) versus ln(V) in LRS and HRS of HfO_x/BN device.

The schematic diagrams of band structure for HfO_x and HfO_x/BN bilayer devices are shown in Fig. 9. Electrons are ejected from TiN electrode and fill into the HfO_x layer, which results in the formation of oxygen filament[19] as shown in Fig. 9(a). The low permittivity BN film acts as a barrier layer for the injecting electrons, and thus resulting in the filament with less oxygen vacancies as shown in Fig. 9(b). The restriction of oxygen filament increases the value of LRS and leads to the low power consumption. With the increase of BN thickness, the barrier for injecting the electrons from TiN electrode into HfO_x layer becomes higher, so the higher LRS is achieved. In the following reset process, the higher LRS leads to the decrease of reset current. This is the reason why reset current decreases with BN thickness increasing. The formation and rupture of less oxygen vacancies' filament also reduce the randomness of the resistive switching process and improve the uniformity.

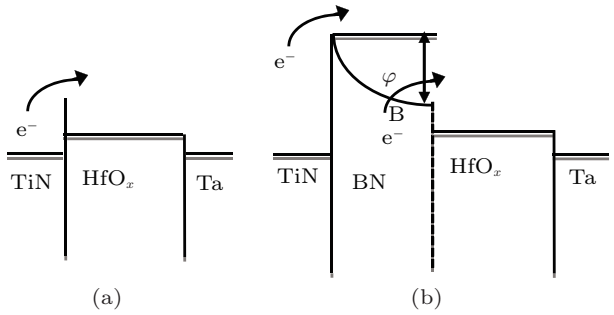


Fig. 9. Schematic diagrams of band structure for (a) Ta/HfO_x/TiN device and (b) Ta/HfO_x/BN/TiN device.

4. Conclusions

In this work, the resistive switching uniformity and low-power consumption features are greatly improved in the HfO_x-based RRAM by inserting a thin BN layer between HfO_x and the TiN bottom electrode. The super-smooth, low-permittivity, and high-resistivity BN thin film layer acts as a barrier layer for injecting the electrons and localizes the oxygen filament in the subsequent switching processes and reduces the reset current. The reset current decreases with BN thickness increasing. The conduction mechanism of the HfO_x/BN bilayer device is believed to be the space-charge-limited current (SCLC) in the LRS while that could be attributed to the Ohmic conduction in the HfO_x device.

References

[1] Liu Q, Sun J, Lv H B, Long S B, Yin K B, Wan N, Li Y T, Sun L T and Liu M 2012 *Adv. Mater.* **24** 1844
[2] Zhao J W, Liu F J, Huang H Q, Hu Z F and Zhang X Q 2012 *Chin. Phys. B* **21** 065201
[3] Waser R and Aono M 2007 *Nat. Mater.* **6** 833
[4] Li Y T, Long S B, Lu H B, Liu Q, Wang Q, Wang Y, Zhang S, Lian WT, Liu S and Liu M 2011 *Chin. Phys. B* **20** 017305
[5] Pan F, Gao S, Chen C, Song C and Zeng F 2014 *Mater. Sci. Eng. R* **83** 1
[6] Fang Z, Yu H Y, Li X, Singh N, Lo G Q and Kwong D L 2011 *IEEE Electron Dev. Lett.* **32** 566
[7] Wen X Z, Chen X, Wu N J and Ignatiev A 2011 *Chin. Phys. B* **20** 097703
[8] Meng Y, Zhang P J, Liu Z Y, Liao Z L, Pan X Y, Liang X J, Zhao H Wand Chen D M 2010 *Chin. Phys. B* **19** 037304
[9] Zhang K L, Liu K, Wang F, Yin F H, Wei X Y and Zhao J S 2013 *Chin. Phys. B* **22** 097101
[10] Gao S, Zeng F, Wang M J, Wang G Y, Song C and Pan F 2015 *Sci. Rep.* **5** 15467

[11] Gao S, Zeng F, Li F, Wang MJ, Mao H J, Wang G Y, Song C and Pan F 2015 *Nanoscale* **7** 6031
[12] Raghavan N, Pey K L, Li X, Liu W H, Wu X, Bosman M and Kauerauf T 2011 *IEEE Electron Dev. Lett.* **32** 716
[13] Song Y L, Liu Y, Wang Y L, Wang M, Tian X P, Yang L M and Lin Y Y 2011 *IEEE Electron Dev. Lett.* **32** 1439
[14] Yu S M, Gao B, Dai H B, Sun B, Liu L F, Liu X Y, Han R Q, Kang J F and Yu B 2010 *Electrochem. Solid State Lett.* **13** H36
[15] Zhao Q, Zhou M X, Zhang W, Liu Q, Li X F, Liu M and Dai Y H 2013 *J. Semicond.* **34** 032001
[16] Liu X, Sadaf S M, Kim S, Biju K P, Cao X, Son M, Choudhury S H, Jung G Y and Hwang H 2012 *ECS Solid State Lett.* **1** Q35
[17] Huang J W, Zhang R, Chang T C, Tsai T M, Chang K C, Lou J C, Young T F, Chen J H, Chen H L,Pan Y C, Huang X, Zhang F Y, Syu Y E and Simon M S 2013 *Appl. Phys. Lett.* **102** 203507
[18] Lei X Y, Liu H X, Gao H X, Yang H N, Wang G M, Long S B, Ma X H and Liu M 2014 *Chin. Phys. B* **23** 117305
[19] Lee D, Woo J, Park S, Cha E, Lee S and Hwang H 2014 *Appl. Phys. Lett.* **104** 083507